HHS Public Access

Author manuscript

Angew Chem Int Ed Engl. Author manuscript; available in PMC 2023 February 21.

Published in final edited form as:

Angew Chem Int Ed Engl. 2022 February 21; 61(9): e202115846. doi:10.1002/anie.202115846.

Optical Control of Mitosis with a Photoswitchable Eg5 Inhibitor

Anna C. Impastato[a,#], **Andrej Shemet**[a,#], **Nynke A. Vepřek**[a,b], **Gadiel Saper**[c], **Lu Rao**[d], **Henry Hess**[c], **Arne Gennerich**[d], **Dirk Trauner**[a]

[a]Department of Chemistry, New York University, New York, 10003, USA

[b]Department of Chemistry, Ludwig-Maximilians University of Munich, 81377 Munich, Germany

[c]Department of Biomedical Engineering, Columbia University, New York, 10025, USA

[d]Department of Anatomy and Structural Biology, Albert Einstein College of Medicine, New York, 10461, USA

Abstract

Eg5 is a kinesin motor protein that is responsible for bipolar spindle formation and plays a crucial role during mitosis. Loss of Eg5 function leads to the formation of monopolar spindles, followed by mitotic arrest, and subsequent cell death. Several cell-permeable small molecules have been reported to inhibit Eg5 and some have been evaluated as anticancer agents. We now describe the design, synthesis, and biological evaluation of photoswitchable variants with five different pharmacophores. Our lead compound **Azo-EMD** is a cell permeable azobenzene that inhibits Eg5 more potently in its light-induced cis form. This activity decreased movement in microtubule gliding assays, promoted formation of monopolar spindles, and led to mitotic arrest in a light dependent way.

Graphical Abstract

The optical control of a mitotic kinesin, Eg5, was achieved through an azobenzene analog of EMD-534085. Under UV light conditions, HeLa cells undergo mitotic arrest, as evidenced by the formation of a monopolar spindle.

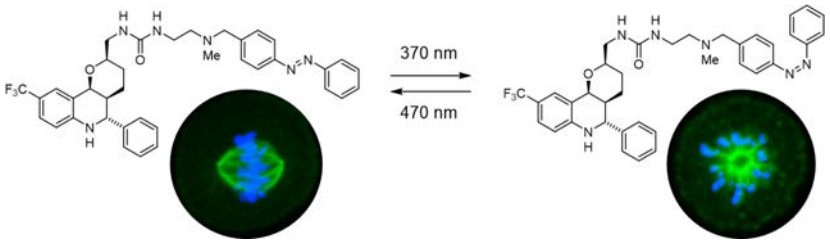

Keywords

photopharmacology; motor proteins; Povarov multicomponent reaction; cytoskeleton

dirktrauner@nyu.edu, arne.gennerich@einsteinmed.edu.

[#]These authors contributed equally to this work.

Supporting information for this article is given via a link at the end of the document.

Mitosis followed by cytokinesis is the process in which a replicated set of chromosomes is evenly distributed, and a single cell is divided into two daughter cells. Hundreds of proteins are involved in this highly complex but tightly controlled event[1], including, amongst other mitotic kinesins, the kinesin spindle protein (KSP, KIF11, or Eg5)[2]. Eg5 is a motor protein that is primarily responsible for generating the forces necessary to organize spindles and separate the centrosomes[3]. Structurally, Eg5 is a homotetramer, which crosslinks and slides apart antiparallel microtubules. Mechanistically, it moves along the microtubules by repetition of an ATP hydrolysis-driven cycle of attachment, sliding, and dissociation[4]. Eg5 specific inhibitors cause cell cycle arrest and apoptotic cell death with a characteristic monopolar spindle phenotype, thus underscoring the importance of this protein during mitosis[5] (Fig. 1A).

Due to their key roles in cell proliferation, mitotic kinesins have emerged as targets in cancer therapy.[6] Their inhibition results in mitotic arrest without directly affecting microtubule dynamics. As such, Eg5 inhibitors provide an alternative mode of inhibition to taxanes and vinca alkaloids[7], molecules that also affect microtubules in non-dividing cells and can cause serious side effects. In the past decades, several small molecules that target Eg5, such as monastrol[5], S-trityl-L-cysteine[8], ispinesib[9], and filanesib[10], have been investigated as potential cancer therapeutics[11] (Fig. 1B). These allosteric Eg5 inhibitors bind to a hydrophobic pocket and prevent ADP release by forming a ternary complex with the protein and ADP[12–14]. To date, at least nine Eg5 inhibitors have progressed through Phase I/II clinical trials, however their development has been stopped due to poor clinical responses[11,15–21].

Photopharmacology is an attempt to control biological activity with synthetic light-responsive molecules[22–25]. It has been applied to neuroreceptors[26], enzymes[27–31], and elements of the cytoskeleton. For instance, tubulin and actin dynamics were modulated with photoswitchable versions of combretastatin A[32–34], paclitaxel[35], and jasplakinolide[36], respectively. However, this approach has rarely been attempted with motor proteins. The Tamaoki group introduced one of the first photoswitchable inhibitors of a motor protein for the mitotic kinesin CENP-E, which was based on the small molecule GSK923295[37,38]. Recently, Maruta and colleagues introduced photoswitchable inhibitors that enabled reversible control of Eg5 *in vitro.*[39–41] However, they did not demonstrate activity in cells, possibly due to insufficient cell permeability and solubility of their compounds. This led us to synthesize and evaluate azobenzene-based photoswitchable Eg5 inhibitors. We aimed to identify compounds that were inactive in the dark-adapted *trans*-form and would become active in the light activated *cis*-form.

We now report the design, synthesis, and systematic evaluation of photoswitchable Eg5 kinesin inhibitors that can permeate membranes and function in cells. We based our approach on five different Eg5 pharmacophores: ispinesib[9], S-trityl-L-cysteine (STLC)[8], monastrol[5], tetrahydro-β-carbolines[42], and EMD-534085[43]. This resulted in the photoswitchable molecules **1a-c**, derived from monastrol, **2a-c**, derived from ispinesib, **3**, modelled after STLC, **4a,b** derived from a class of β-carboline inhibitors, and **5a-c**, derived from EMD-534085. Amongst these, **5c**, also termed **Azo-EMD** emerged as the most successful.

The design of photoswitchable compounds was based on structure-activity data available for various Eg5 inhibitors and the analysis of X-ray structures of monastrol (pdb 1X88), ispinesib (pdb 4AP0), and EMD-534085 (pdb 3L9H) bound to Eg5. These inhibitors bind to the same allosteric site, which is about 10 Å away from the ATP binding pocket in a region formed by helix α2/loop L5 and helix α3. The accommodation of structurally different compounds in the same binding pocket implies that Eg5 exhibits some degree of flexibility to allow for conformational changes upon binding of ligand. Keeping this in mind, we opted for an azo-extension[22] approach, where an azobenzene is appended to a vector that projects toward solvent and can accommodate the photoswitch. This led us to synthesize and evaluate azobenzene derivatives **1–5** (Fig. 2).

The syntheses of compounds **1a-c**, **2a-c**, **3**, and **4a,b** is described in the Supporting Information. The racemic synthesis[44] of our lead compound **Azo-EMD** commenced with a Povarov multi-component reaction[45] (Scheme 1B). It provided access to the tetrahydroquinoline core containing three stereocenters in a single step starting from commercially available materials. The relative configuration was confirmed by X-ray crystallography (see Supporting Information.) Following a few steps to convert the alcohol to the amine, the azobenzene photoswitch functionality was introduced using a CDI mediated urea coupling. In addition to the *para* substituted derivative **Azo-EMD** (**5c**) we also synthesized *ortho* and *meta* substituted variants by coupling the common building block **12** with CDI and the corresponding azobenzyl amine (Scheme 1A). All of the analogs show photochemical properties expected of classic azobenzene photoswitches[46]. **Azo-EMD** can be reversibly switched from the *trans* to *cis* configuration using alternating 365 and 465 nm light (Scheme 1D,E). Once switched to the *cis* configuration, **Azo-EMD** is bi-stable and has a long thermal half-life of 27 hours at 37 °C. (Fig. 1D and Supporting Information). As expected, the switching could be repeated over several cycles without fatigue (Fig. 1E). Interestingly, in the dark-adapted state Azo-EMD adopts a *cis:trans* of 13:87, which could not be further increased. Upon irradiation with 370 nm a photostationary state (PSS) of 95:5 could be obtained (Figure 1F).

Since Eg5-inhibition ultimately results in cell death[47], we first screened our photoswitchable compounds in cell viability assays (Fig. 3A, Supporting Information). HeLa cells were treated for 48 hours with each respective photoswitch under dark or pulsed-light conditions (repeated 75 ms pulse of light every 15 s over 48h). Monastrol derivatives **1a-c** were either not cytotoxic or their cytotoxicity was not light dependent. The usefulness of these compounds was also limited by the concentrations that could be tested due to their poor solubility. Ispinesib derivatives **2a-b** showed some cytotoxicity (60% cell viability at 100 μM) however, the concentrations tested could not be increased without observing compound precipitation. The secondary amine proved to be critical for Eg5 inhibition, consistent with the reported structure activity relationships of ispinesib analogs[48]. Accordingly, **2c,** which maintains the secondary amine, proved to be a potent inhibitor (IC_{50} = 7.6 nM), however the activity of **2c** was not light dependent. S-trityl cysteine derivate **3** was inactive, showing no effects on cell viability. THBC derivates **4a,b** were active inhibitors but not in a light-dependent way.

EMD-534085 derivates, **5a-c**, on the other hand, were active and showed light dependency in the cell viability assays**. 5a** and **Azo-EMD** (**5c**) were the most potent and showed similar cytotoxicity in their *cis*-enriched forms. **5b** was relatively less cytotoxic compared with **5a** and **5c**. We decided to evaluate **Azo-EMD (5c)** in further biological experiments because it showed the largest difference in IC_{50} between *cis* and *trans* isomers.

Cell cycle analysis by DNA content showed that treatment with *cis* **Azo-EMD** (3 μM, 370 nm pulsed irradiation, 75 ms pulse every 15 sec for 24 h) induced a strong shift towards the G2/M phases (Figure 3 B,C). In comparison, cells treated with *trans* **Azo-EMD** in the dark (3 μM, 24 h) did not show a shift in cell cycle populations compared with co-solvent treated cells. In agreement with the cell viability assays, the cell cycle analysis therefore shows that **Azo-EMD** is *cis*-active. This effect is dose-dependent, and the largest difference in effect between light and dark treated samples is seen at 3 μM (see Supporting Information). The shift in cell cycle population towards G2/M is consistent with the observed effects of Eg5 inhibitors, such as EMD-534085 (Figure 3B,C), monastrol[5], and filanesib[10].

The motor function of a single Eg5 dimer can be observed using total internal reflection fluorescence (TIRF) microscopy. While Eg5 forms a homotetramer in cells, it is the two motor domains of each incorporated Eg5 dimer located at opposite ends of the tetramer that move processively along anti-parallel microtubules to slide them apart. Stabilized microtubules are bound to a coverslip and fluorescent Eg5 constructs are able to move processively along the microtubules[49]. The movement of Eg5 (1–531) motors was minimally affected when 3 μM **Azo-EMD** in either the dark-adapted or pre-irradiated with 465 nm light was added (Figure 4). When the motors are treated with 3 μM *cis* Azo-EMD (pre-irradiated with 365 nM light), the movement was significantly reduced. The effects of *cis*-Azo-EMD on Eg5 motor function were dose-dependent (Supporting Information). These data show that *cis* Azo-EMD directly inhibits Eg5 motors.

We estimated the microtubule-stimulated ATP-hydrolysis rates of Eg5 in the absence and presence of 3 μM preactivated Azo-EMD directly from the velocities we obtained from the single-molecule TIRF assay. The measured velocities and calculated ATPase rates for 1 and 10 μM Azo-EMD concentrations are given in Supplemental Figure 6 and Supplemental Table 1. Given that Eg5 takes only 8 nm forward steps under low load[50] and that ATP hydrolysis triggers the forward stepping of kinesin motors[51,52], we can estimate the ATPase rates directly from the measured velocities. Our analysis shows that 3 μM preactivated Azo-EMD reduces the microtubule-activated ATPase rates of Eg5 by 35.7% from 2.8/s to 1.8/s. Our analyses are therefore consistent with the predicted effects of the inhibitor.

Finally, we evaluated Azo-EMD in fluorescence imaging assays to confirm that the observed effects on cell viability and the cell cycle are due to monopolar spindle formation caused by Eg5 inhibition[5] (Figure 5). In the presence of **Azo-EMD** (1 μM) and in the absence of irradiation, most cells show the normal bipolar spindle phenotype, which is observed as the linear arrangement of the stained chromosomes. By contrast, upon pulse-irradiation with 370 nm light (75 ms pulse, every 15 s), most dividing cells show the monoastral phenotype, corresponding to Eg5 inhibition, where the chromatin is arranged radially. HeLa cells treated

with EMD-534085 (1 μM) exhibit the characteristic monopolar spindle both in the dark and under pulsed 370 nm irradiation.

To explain the observed differences between *cis* and *trans* **Azo-EMD**, we performed molecular docking studies using the crystal structure of EMD-534085 bound to the Eg5 motor domain (pdb 3L9H, Supporting Information). While the differences are not large, the calculated docking score for *cis* **Azo-EMD** (glide score = –9.8) is lower than the docking score for *trans* **Azo-EMD** (glide score = –8.1). The difference in docking scores is due to improved hydrophobic interactions of the *cis* Azo-EMD with the protein. These results are consistent with our experimental results.

In summary, we have described the design, synthesis, and biological evaluation of a photoswitchable and cell permeable Eg5 inhibitor, termed **Azo-EMD.** At an appropriate concentration **Azo-EMD** is inactive in the dark, is activated by irradiation with UV-A light, and enables the optical control of Eg5-dependent biology. The long thermal half-lives, coupled with poor photostationary states, prevent the effects of **Azo-EMD** from being reversible in cellular assays. Future work will involve optimizing these parameters. The optical control of kinesin function can also be achieved using optogenetics[53–55]. To the best of our knowledge, however, the optogenetic control of Eg5 itself has not been achieved. A photoswitchable Eg5 inhibitor with cellular activity could provide a useful tool for studying the role of the kinesin with high spatial and temporal precision. Additionally, localized and reversible control of Eg5 at different phases of the cell cycle may serve to probe the directional forces involved in centrosome separation. Since the photostationary states of photoswitches are a function of the wavelength used, the concentration of the active form can be changed *in situ* (colordosing)[32]. Light-activatable Eg5 inhibitors, such as **Azo-EMD**, could also be interesting candidates for precision cancer chemotherapeutics that can avoid systemic toxicity which has hampered the clinical development of Eg5 inhibitors[21].

Supplementary Material

Refer to Web version on PubMed Central for supplementary material.

Acknowledgements

A.C.I. is supported by the NYU MacCracken Fellowship. A.S. thanks the Swiss National Science Foundation (SNSF) for a postdoctoral fellowship (P2EZP_181623). N.A.V. thanks the German Academic Scholarship Foundation (Studienstiftung) for a PhD Fellowship. G.S. and H.H. are supported by NSF grant 1807514. This research was supported by the National Institute of General Medical Sciences of the National Institutes of Health under award number R01GM126228 (to D.T.). L.R. and A.G. are supported by National Institutes of Health (NIH) grants R01GM098469 and R01NS114636. We are grateful to Dr. Michelle C. Neary (Hunter College, New York) for X-ray crystallographic analysis of 11a.

References

[1]. O'Connor C, Nature Education 2008, 1, 188.

[2]. Wordeman L, Semin Cell Dev Biol 2010, 21, 260–268. [PubMed: 20109570]

[3]. Mann BJ, Wadsworth P, Trends in Cell Biology 2019, 29, 66–79. [PubMed: 30220581]

[4]. Valentine MT, Gilbert SP, Current Opinion in Cell Biology 2007, 19, 75–81. [PubMed: 17188855]

[5]. Mayer TU, Kapoor TM, Haggarty SJ, King RW, Schreiber SL, Mitchison TJ, Science 1999, 286, 971–974. [PubMed: 10542155]

[6]. Rath O, Kozielski F, Nat Rev Cancer 2012, 12, 527–539. [PubMed: 22825217]

[7]. Jordan MA, Wilson L, Nat Rev Cancer 2004, 4, 253–265. [PubMed: 15057285]

[8]. DeBonis S, Skoufias DA, Indorato R-L, Liger F, Marquet B, Laggner C, Joseph B, Kozielski F, J. Med. Chem 2008, 51, 1115–1125. [PubMed: 18266314]

[9]. Lad L, Luo L, Carson JD, Wood KW, Hartman JJ, Copeland RA, Sakowicz R, Biochemistry 2008, 47, 3576–3585. [PubMed: 18290633]

[10]. Carter BZ, Mak DH, Woessner R, Gross S, Schober WD, Estrov Z, Kantarjian H, Andreeff M, Leukemia 2009, 23, 1755–1762. [PubMed: 19458629]

[11]. Garcia-Saez I, Skoufias DA, Biochemical Pharmacology 2021, 184, 114364. [PubMed: 33310050]

[12]. Nagarajan S, Sakkiah S, Journal of Biomolecular Structure and Dynamics 2019, 37, 2394–2403. [PubMed: 30047307]

[13]. Behnke-Parks WM, Vendome J, Honig B, Maliga Z, Moores C, Rosenfeld SS, Journal of Biological Chemistry 2011, 286, 5242–5253. [PubMed: 21148480]

[14]. Kaan HYK, Major J, Tkocz K, Kozielski F, Rosenfeld SS, J. Biol. Chem 2013, 288, 18588–18598. [PubMed: 23658017]

[15]. O'Connor OA, Gerecitano J, Deventer HV, Hainsworth J, Zullo KM, Saikali K, Seroogy J, Wolff A, Escandón R, Leukemia & Lymphoma 2015, 56, 2585–2591. [PubMed: 25665464]

[16]. Hollebecque A, Deutsch E, Massard C, Gomez-Roca C, Bahleda R, Ribrag V, Bourgier C, Lazar V, Lacroix L, Gazzah A, Varga A, de Baere T, Beier F, Kroesser S, Trang K, Zenke FT, Klevesath M, Soria J-C, Invest New Drugs 2013, 31, 1530–1538. [PubMed: 24077982]

[17]. Khoury HJ, Garcia-Manero G, Borthakur G, Kadia T, Foudray MC, Arellano M, Langston A, Bethelmie-Bryan B, Rush S, Litwiler K, Karan S, Simmons H, Marcus AI, Ptaszynski M, Kantarjian H, Cancer 2012, 118, 3556–3564. [PubMed: 22139909]

[18]. Wakui H, Yamamoto N, Kitazono S, Mizugaki H, Nakamichi S, Fujiwara Y, Nokihara H, Yamada Y, Suzuki K, Kanda H, Akinaga S, Tamura T, Cancer Chemother Pharmacol 2014, 74, 15–23. [PubMed: 24752449]

[19]. Jones R, Vuky J, Elliott T, Mead G, Arranz JA, Chester J, Chowdhury S, Dudek AZ, Müller-Mattheis V, Grimm M-O, Gschwend JE, Wülfing C, Albers P, Li J, Osmukhina A, Skolnik J, Hudes G, Invest New Drugs 2013, 31, 1001–1007. [PubMed: 23329066]

[20]. Kantarjian HM, Padmanabhan S, Stock W, Tallman MS, Curt GA, Li J, Osmukhina A, Wu K, Huszar D, Borthukar G, Faderl S, Garcia-Manero G, Kadia T, Sankhala K, Odenike O, Altman JK, Minden M, Invest New Drugs 2012, 30, 1107–1115. [PubMed: 21494838]

[21]. Indorato R-L, Talapatra SK, Lin F, Haider S, Mackay SP, Kozielski F, Skoufias DA, Mol Cancer Ther 2019, 18, 2394–2406. [PubMed: 31488701]

[22]. Broichhagen J, Frank JA, Trauner D, Acc. Chem. Res 2015, 48, 1947–1960. [PubMed: 26103428]

[23]. Hüll K, Morstein J, Trauner D, Chem. Rev 2018, 118, 10710–10747. [PubMed: 29985590]

[24]. Fuchter MJ, J. Med. Chem 2020, 63, 11436–11447. [PubMed: 32511922]

[25]. Velema WA, Szymanski W, Feringa BL, J. Am. Chem. Soc 2014, 136, 2178–2191. [PubMed: 24456115]

[26]. Szobota S, Isacoff EY, Annual Review of Biophysics 2010, 39, 329–348.

[27]. Matsuo K, Thayyil S, Kawaguchi M, Nakagawa H, Tamaoki N, Chemical Communications 2021, 57, 12500–12503. [PubMed: 34751279]

[28]. Hoorens MWH, Ourailidou ME, Rodat T, van der Wouden PE, Kobauri P, Kriegs M, Peifer C, Feringa BL, Dekker FJ, Szymanski W, European Journal of Medicinal Chemistry 2019, 179, 133–146. [PubMed: 31252305]

[29]. Schehr M, Ianes C, Weisner J, Heintze L, Müller MP, Pichlo C, Charl J, Brunstein E, Ewert J, Lehr M, Baumann U, Rauh D, Knippschild U, Peifer C, Herges R, Photochem. Photobiol. Sci 2019, 18, 1398–1407. [PubMed: 30924488]

[30]. Ferreira R, Nilsson JR, Solano C, Andréasson J, Grøtli M, Sci Rep 2015, 5, 9769. [PubMed: 25944708]

[31]. Vomasta D, Högner C, Branda NR, König B, Angewandte Chemie International Edition 2008, 47, 7644–7647. [PubMed: 18767093]

[32]. Borowiak M, Nahaboo W, Reynders M, Nekolla K, Jalinot P, Hasserodt J, Rehberg M, Delattre M, Zahler S, Vollmar A, Trauner D, Thorn-Seshold O, Cell 2015, 162, 403–411. [PubMed: 26165941]

[33]. Gao L, Meiring JCM, Kraus Y, Wranik M, Weinert T, Pritzl SD, Bingham R, Ntouliou E, Jansen KI, Olieric N, Standfuss J, Kapitein LC, Lohmüller T, Ahlfeld J, Akhmanova A, Steinmetz MO, Thorn-Seshold O, Cell Chemical Biology 2021, 28, 228–241.e6. [PubMed: 33275880]

[34]. Sailer A, Ermer F, Kraus Y, Bingham R, Lutter FH, Ahlfeld J, Thorn-Seshold O, Beilstein J. Org. Chem 2020, 16, 125–134. [PubMed: 32082431]

[35]. Müller-Deku A, Meiring JCM, Loy K, Kraus Y, Heise C, Bingham R, Jansen KI, Qu X, Bartolini F, Kapitein LC, Akhmanova A, Ahlfeld J, Trauner D, Thorn-Seshold O, Nat Commun 2020, 11, 4640. [PubMed: 32934232]

[36]. Borowiak M, Küllmer F, Gegenfurtner F, Peil S, Nasufovic V, Zahler S, Thorn-Seshold O, Trauner D, Arndt H-D, J. Am. Chem. Soc 2020, 142, 9240–9249. [PubMed: 32388980]

[37]. Mafy NN, Matsuo K, Hiruma S, Uehara R, F N, J. Am. Chem. Soc 2020, 142, 1763–1767. [PubMed: 31927956]

[38]. Matsuo K, Tamaoki N, Organic & Biomolecular Chemistry 2021, 19, 6979–6984. [PubMed: 34346473]

[39]. Ishikawa K, Tamura Y, Maruta S, Journal of Biochemistry 2014, 155, 195–206. [PubMed: 24334276]

[40]. Sadakane K, Alrazi IMD, Maruta S, The Journal of Biochemistry 2018, 164, 295–301. [PubMed: 29860530]

[41]. Alrazi IMD, Sadakane K, Maruta S, The Journal of Biochemistry 2021, mvab035.

[42]. Barsanti PA, Wang W, Ni Z-J, Duhl D, Brammeier N, Martin E, Bussiere D, Walter AO, Bioorganic & Medicinal Chemistry Letters 2010, 20, 157–160. [PubMed: 19945875]

[43]. Schiemann K, Finsinger D, Zenke F, Amendt C, Knöchel T, Bruge D, Buchstaller H-P, Emde U, Stähle W, Anzali S, Bioorganic & Medicinal Chemistry Letters 2010, 20, 1491–1495. [PubMed: 20149654]

[44]. Schiemann K, Emde U, Schlueter T, Saal C, Maiwald M, POLYMORPHIC FORMS AND PROCESS, n.d., US 8,198.452 B2.

[45]. Povarov LS, Russ. Chem. Rev 1967, 36, 656–670.

[46]. Sadovski O, Beharry AA, Zhang F, Woolley GA, Angewandte Chemie International Edition 2009, 48, 1484–1486. [PubMed: 19148911]

[47]. Marcus AI, Peters U, Thomas SL, Garrett S, Zelnak A, Kapoor TM, Giannakakou P, J. Biol. Chem 2005, 280, 11569–11577. [PubMed: 15653676]

[48]. Good JAD, Berretta G, Anthony NG, Mackay SP, in Kinesins and Cancer (Ed.: Kozielski Frank F), Springer Netherlands, Dordrecht, 2015, pp. 27–52.

[49]. Nicholas MP, Rao L, Gennerich A, in Mitosis: Methods and Protocols (Ed.: Sharp DJ), Springer, New York, NY, 2014, pp. 137–169.

[50]. Valentine MT, Fordyce PM, Krzysiak TC, Gilbert SP, Block SM, Nat Cell Biol 2006, 8, 470–476. [PubMed: 16604065]

[51]. Zaniewski TM, Gicking AM, Fricks J, Hancock WO, Journal of Biological Chemistry 2020, 295, 17889–17903. [PubMed: 33082143]

[52]. Hancock WO, Biophysical Journal 2016, 110, 1216–1225. [PubMed: 27028632]

[53]. van Bergeijk P, Adrian M, Hoogenraad CC, Kapitein LC, Nature 2015, 518, 111–114. [PubMed: 25561173]

[54]. Nijenhuis W, van Grinsven MMP, Kapitein LC, J Cell Biol 2020, 219, e201907149.

[55]. Zhang H, Aonbangkhen C, Tarasovetc EV, Ballister ER, Chenoweth DM, Lampson MA, Nat Chem Biol 2017, 13, 1096–1101. [PubMed: 28805800]

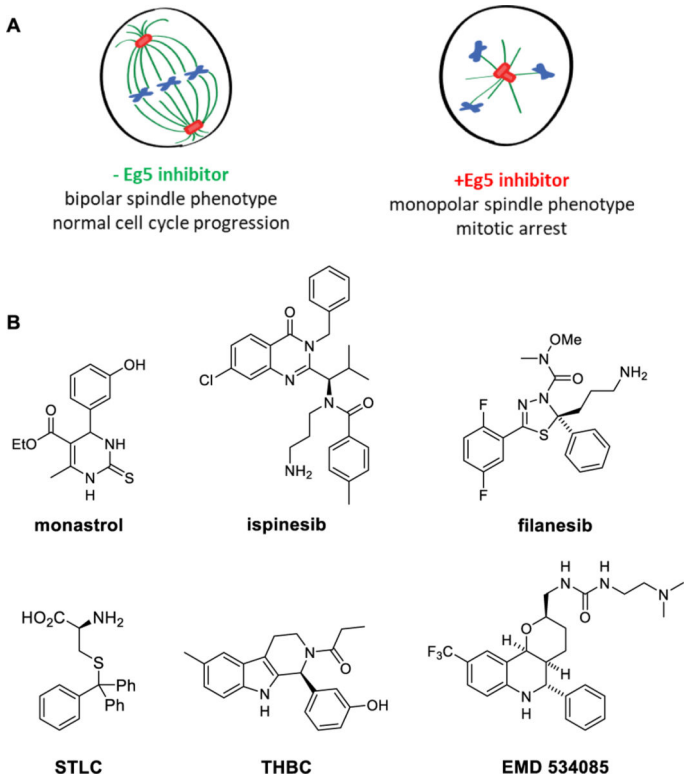

Figure 1.

A) Eg5 is involved in the formation of the bipolar spindle during mitosis. When its function is inhibited, monopolar spindle formation is observed, which is followed by subsequent mitotic arrest. B) Structural diversity of allosteric Eg5 inhibitors.

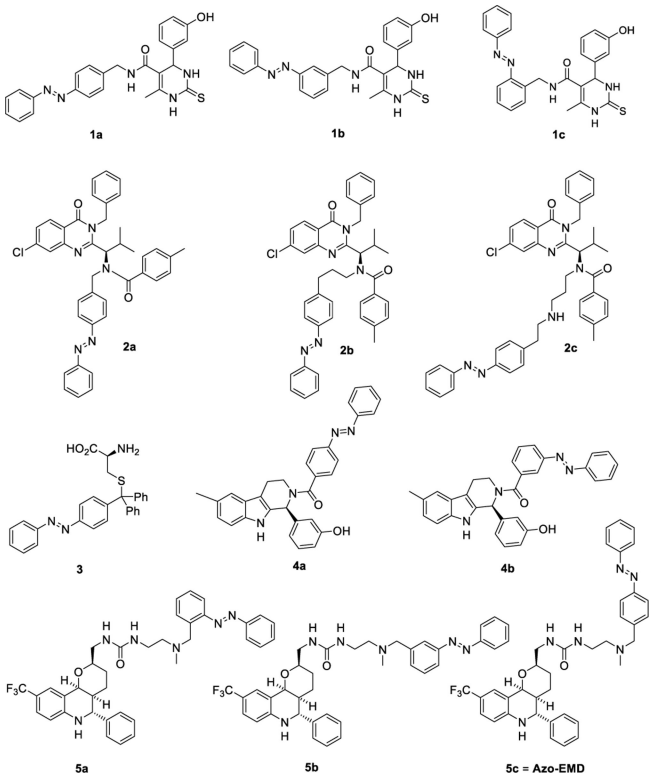

Figure 2.

Photoswitchable inhibitors of Eg5 synthesized and tested in this study were based on the pharmacophores of monastrol, ispinesib, STLC, and EMD-534085.

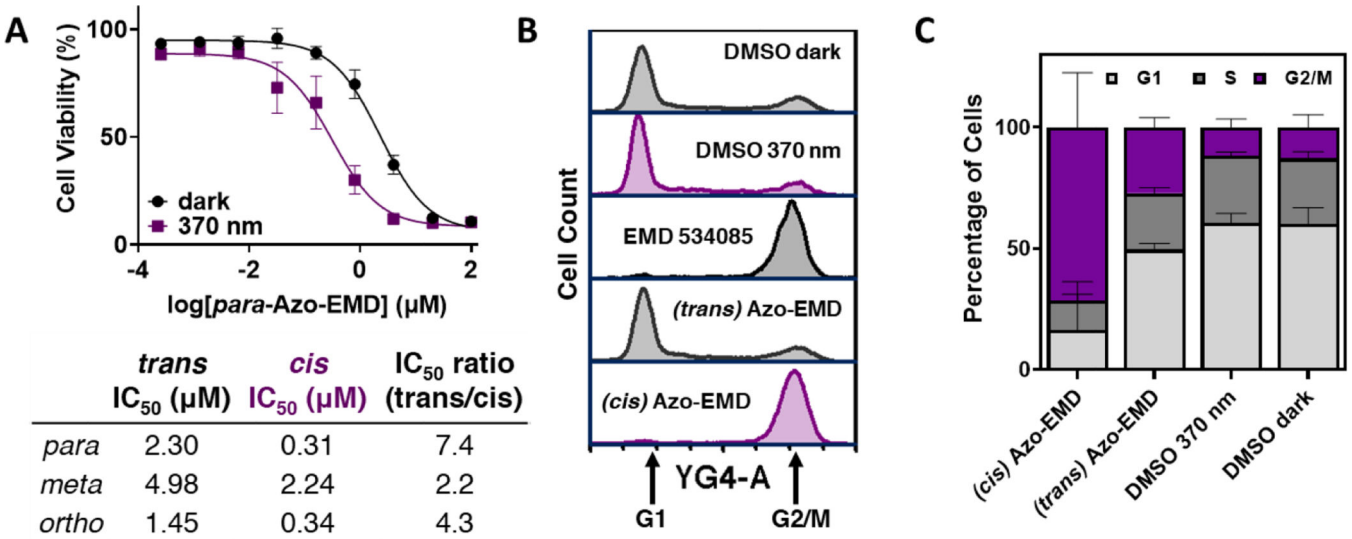

	trans IC_{50} (μM)	*cis* IC_{50} (μM)	IC_{50} ratio (trans/cis)
para	2.30	0.31	7.4
meta	4.98	2.24	2.2
ortho	1.45	0.34	4.3

Figure 3.

A) Cell viability assay: HeLa cells were treated with increasing concentrations of compound under dark or pulsed irradiation conditions for 48 h and cell viability was assessed using MTT assays. n=3, N=3; B, C) Cell cycle distribution of HeLa cells treated with Azo-EMD (3 μM), EMD-534085 (0.1 μM), or DMSO under dark or pulsed irradiation (75 ms pulse every 15 sec) for 24 h. Cells were fixed in EtOH, stained with propidium iodide and analyzed by flow cytometry. N=3. Data shown are mean values ± SD.

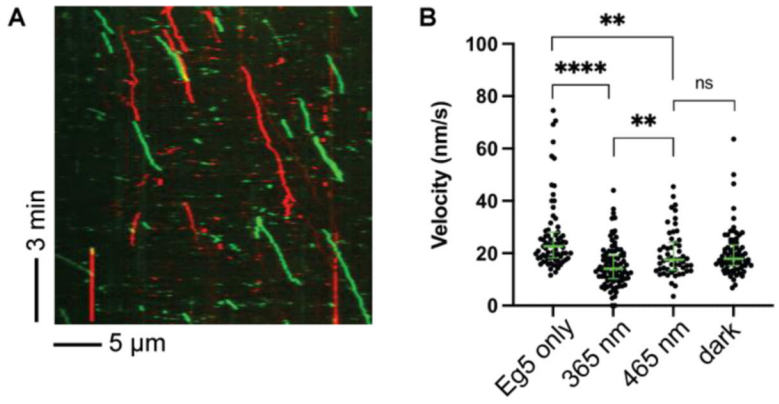

Figure 4.

A) Overlaid kymographs of Eg5 only (green) and Eg5 with 3 μM pre-activated Azo-EMD (red) moving along microtubules. B) Velocities of Eg5 only (Eg5 only), Eg5 with 3 μM pre-activated Azo-EMD (365 nm), Eg5 with 3 μM Azo-EMD, pre-irradiated with 465 nm, and Eg5 with 3 μM dark adapted Azo-EMD (dark). The green bars represent the median with quartiles. Eg5 only: 22.6 [18.2, 28] nm/s; 365 nm: 14.1 [10.2, 19.1] nm/s; 465 nm: 17.6 [13.6, 24.0] nm/s; Dark: 17.9 [15.3, 23.1] nm/s. Unpaired *t*-test were performed (****, $p < 0.0001$; **, $p < 0.01$; ns, $p > 0.05$).

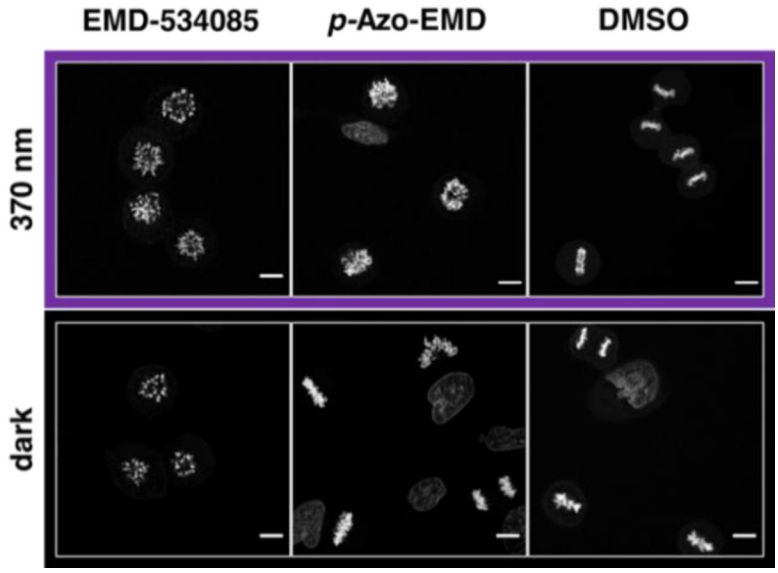

Figure 5.

Synchronized HeLa cells were treated with EMD-534085 (1 μM), Azo-EMD (1 μM) or DMSO under dark or pulsed irradiation (370 nm LED array, 75 ms pulse every 15 s), followed by fixation, permeabilization and staining. Scale bar 10 μm. **Middle:** Azo-EMD shows mostly regular mitotic phenotype under dark conditions and upon activation (370 nm) the star-like DNA phenotype that is a consequence of monopolar spindle formation is observed. **Left/Right**: +/– control.

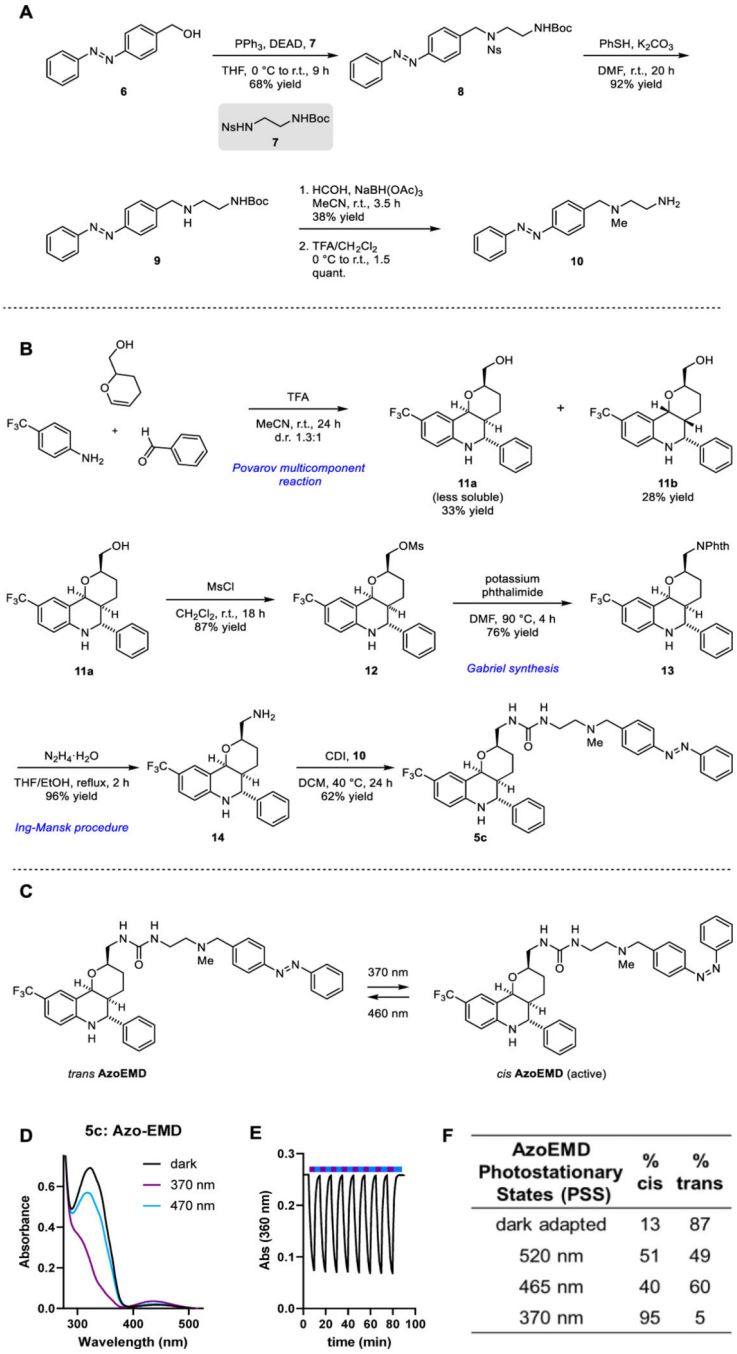

Scheme 1.

A) Synthesis of the photoswitchable side chain **B**. B) Synthesis of Azo-EMD. C) Light-dependent reversible isomerization of Azo-EMD. D) Absorption spectra of photoswitchable EMD-534085 in the dark-adapted state and at 370 and 460 nm. E) Reversible isomerization of Azo-EMD over multiple switching cycles. F) Photostationary states of Azo-EMD.